

# DiffLM: Controllable Synthetic Data Generation via Diffusion Language Models

Ying Zhou<sup>1,2\*</sup>, Xinyao Wang<sup>3\*†</sup>, Yulei Niu<sup>3‡</sup>, Yaojie Shen<sup>1,2</sup>, Lexin Tang<sup>3</sup>, Fan Chen<sup>3</sup>,  
Ben He<sup>1,2‡</sup>, Le Sun<sup>2</sup>, Longyin Wen<sup>3‡</sup>

<sup>1</sup>University of Chinese Academy of Sciences, Beijing, China

<sup>2</sup>Chinese Information Processing Laboratory, Institute of Software,  
Chinese Academy of Sciences, Beijing, China

<sup>3</sup>ByteDance Inc., San Jose, USA

zhouying20@mails.ucas.ac.cn

## Abstract

Recent advancements in large language models (LLMs) have significantly enhanced their knowledge and generative capabilities, leading to a surge of interest in leveraging LLMs for high-quality data synthesis. However, synthetic data generation via prompting LLMs remains challenging due to LLMs’ limited understanding of target data distributions and the complexity of prompt engineering, especially for structured formatted data. To address these issues, we introduce DiffLM, a controllable data synthesis framework based on variational autoencoder (VAE), which further (1) leverages diffusion models to reserve more information of original distribution and format structure in the learned latent distribution and (2) decouples the learning of target distribution knowledge from the LLM’s generative objectives via a plug-and-play latent feature injection module. As we observed significant discrepancies between the VAE’s latent representations and the real data distribution, the latent diffusion module is introduced into our framework to learn a fully expressive latent distribution. Evaluations on seven real-world datasets with structured formatted data (i.e., Tabular, Code, and Tool data) demonstrate that DiffLM generates high-quality data, with performance on downstream tasks surpassing that of real data by 2%–7% in certain cases. Data and code are available at <https://github.com/bytedance/DiffLM>.

## 1 Introduction

Data Synthesis has become an indispensable technique in current machine learning research, enabling rapid generation and modification of datasets (Bauer et al., 2024), allowing researchers to experiment with various scenarios and model architectures without the extensive processes associated with real-world data collection. Meanwhile,

with the rapid advancements in large language models (LLMs), recent research in natural language processing (NLP) has increasingly focused on leveraging LLMs for synthetic data generation. Early efforts attempted to fine-tune LLMs to align with real data distributions (Keskar et al., 2019; Anaby-Tavor et al., 2020; Borisov et al., 2023). As the in-context learning capabilities of LLMs have improved, some studies have explored zero-shot or few-shot prompting of LLMs to generate synthetic data (Ye et al., 2022a; Wei et al., 2024).

Despite the progress achieved, generating high-quality synthetic textual data using LLMs remains challenging, particularly for structured data (Josi-foski et al., 2023; Li et al., 2022). First, LLMs often lack a global understanding of the target data distribution when generating synthetic data. Even after fine-tuning, it is difficult to inject information about complex and varied distributions into current LLM architectures, often resulting in outputs with low diversity and instances of data copying (Wu et al., 2024; Yu et al., 2023). Moreover, existing LLM-based synthetic data generation methods typically involve complex pipelines and post-processing mechanisms, such as prompt engineering, multi-agent frameworks, and iterative sampling (Dekoninck et al., 2024; Wu et al., 2024). These complexities hinder the rapid adaptation of LLMs to new tasks, limiting their utility in dynamic research and industrial scenario. Concurrently, the remarkable performance of variational autoencoders (VAEs) and diffusion models in image synthesis tasks (Betker et al., 2023; Rombach et al., 2022) has spurred interest in adapting these techniques to other modalities (Borisov et al., 2023; Li et al., 2022; Gong et al., 2023). Although some works have introduced latent spaces into language models for simple tasks like style transfer or topic generation (Yang and Klein, 2021; Li et al., 2022), our preliminary experiments indicate that directly applying the latent distributions learned by VAEs

\*Equal contribution.

†Work done before joining Amazon AGI.

‡Corresponding authors.

often results in outputs that are unrelated to the real data. Similar issues also have been addressed in prior works (Amani et al., 2024; Havrylov and Titov, 2020; Bowman et al., 2016). This challenges the direct application of these methods in more complex scenarios for synthetic data generation.

To address these challenges, we propose DiffLM, a novel framework that leverages a plug-and-play latent space to provide data distribution information for LLMs during data generation. First, to decouple the learning of real data distributions from the LLM’s training objectives, we develop a latent space using a VAE model to capture external information, mapping samples from the real dataset to latent vectors. However, we observed that sampling points from a Gaussian distribution obtained from naive VAE that cannot generate realistic results. To overcome the poor quality of data generated by sampling from VAE, we employ a latent diffusion method that linearly adds noise to the latent space over time. A denoising network is then trained to learn these noises in the reverse process, reducing efficiency loss in data synthesis due to sampling failures. Finally, we design a soft prompting method to inject latent features into the LLM decoding process, resulting in controllable, high-quality synthetic data. We evaluate our method on seven real-world structured formatted datasets, ranging from relatively simple table synthesis to more complex code and tool synthesis tasks. Experiments demonstrate that DiffLM can generate high-quality results, and ablation studies confirm the effectiveness of each component in our proposed method. The contributions of this paper are threefold:

- **Decoupling Data Distribution Learning:** We proposed a new VAE-based LLM framework for data synthesis, which decouples the learning of real data distribution information from the training objectives of the LLM by introducing the a small projection network.
- **High-Quality Synthetic Data:** Based on our observations, the meticulously designed VAE and diffusion structures effectively model the distribution of real data, enabling the generation of high-quality synthetic data. In all tasks, the quality of the generated data is comparable to or even surpasses that of the real data.
- **Comprehensive Evaluation:** We validate the high quality of data generated by DiffLM across three distinct scenarios and seven datasets, under-

scoring its robustness and adaptability in advancing synthetic data generation for natural language processing.

## 2 Related Works

### Large Language Models for Data Synthesis.

The recent advancement in the generative capabilities of LLMs has motivated numerous exploratory works aiming to leverage these models for data augmentation in areas such as text classification (Ye et al., 2022a; Li et al., 2023), information extraction (Tang et al., 2023; Josifoski et al., 2023), and tabular data generation (Borisov et al., 2023; Xu et al., 2024). A comprehensive survey conducted by Long et al. (2024) proposes a prompt-based generic workflow for synthetic data generation, curation, and evaluation. And multiple advanced works have attempted to fine-tune language models for data synthesis in recent years (Anaby-Tavor et al., 2020; Kumar et al., 2020; Dinh et al., 2022; Borisov et al., 2023; Xu et al., 2024). Specifically, these methods involve fine-tuning LLMs on a small amount of gold data for language modeling, followed by the use of various sampling methods to generate data. However, a major challenge remains in ensuring that synthetic data accurately reflects real-world distributions. Veselovsky et al. (2023) has shown that LLM-generated data can sometimes diverge from actual data distributions, leading to unfaithful representations that may hinder model training. Some studies have explored data selection (Puri et al., 2020) or data augmentation (Ye et al., 2022b) to address this distribution gap, but there remains significant room for improvement.

### Latent Variable Models for Text Generation.

Latent variable models have made significant advances in computer vision in recent years (Yu et al., 2022a; Gu et al., 2022; Luo et al., 2023a; Gulrajani et al., 2017), achieving high-quality generation results, flexibility and effectiveness, as well as robustness to noise perturbations. In particular, latent diffusion models, such as DALL-E (Betker et al., 2023) and Stable Diffusion (Rombach et al., 2022), operate their diffusion processes in a latent space rather than directly in data space, enabling a near-optimal balance between generation quality and computational efficiency. In text generation, several works (Bowman et al., 2016; Kaiser and Bengio, 2018; Havrylov and Titov, 2020; Li et al., 2022; Gu et al., 2023; Borisov et al., 2023; Amani et al., 2024) have attempted to combine latent spaces with

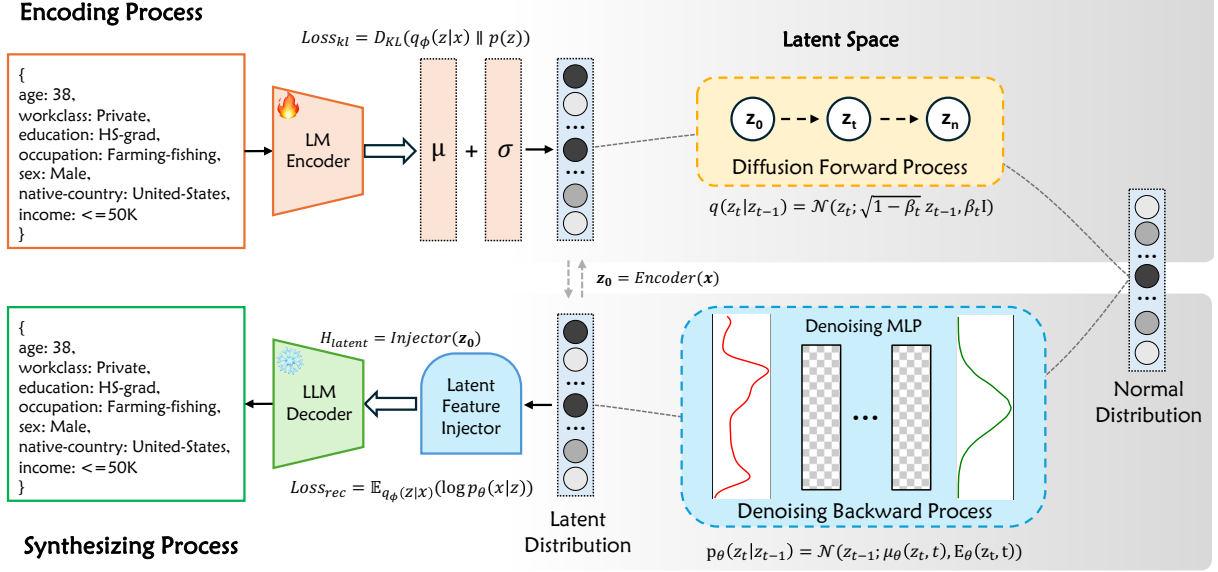


Figure 1: Overview of our **DiffLM**. The trainable language model (LM) works as VAE encoder while the fixed LLM decoder serves as VAE decoder. We further (1) introduced a Diffusion module to learn the latent space, and (2) employ a latent feature injector with soft prompting to align latent vector space with LLM decoder.

language models to accomplish tasks such as language modeling (Lin et al., 2023; Reid et al., 2023; Zhang et al., 2023; Yuan et al., 2024), unconditional text generation (Yu et al., 2022b; Chen et al., 2023) and control text generation (Austin et al., 2021a; He et al., 2023). Additionally, some studies have explored the use of diffusion for plug-and-play controllable generation (Li et al., 2022; Gong et al., 2023), aiming to steer the outputs of pre-trained language model using auxiliary modules. While these works share a similar perspective with ours, we tackle a more challenging scenario of structured data synthesis. To the best of our knowledge, our work is the first to combine VAEs and denoising diffusion models with large language models for high-quality data synthesis.

### 3 Methodology

Figure 1 illustrates the main pipeline of our proposed DiffLM. First, we define an encoder to map discrete text into a continuous latent space (Section 3.2). Second, although the features of the data are extracted and compressed, conventional latent embeddings in text VAEs often lead to decoding failures due to underutilized or empty regions in the latent space. To address this issue, we train a diffusion model on the latent space (Section 3.3). Finally, to incorporate encoded prior knowledge into the decoding stage of large language models, we propose a novel soft prompt injection method

to steer the decoding process (Section 3.4).

#### 3.1 Problem Formulation

We begin by defining  $\mathcal{D}$  as a known small set of real-world distribution data, where each element  $x$  represents a real sample. We define  $G$  as the synthetic data generator, which learns the distribution of  $\mathcal{D}$  and generates a set of synthetic samples,  $\mathcal{D}_{syn}$ , ensuring that the model does not simply memorize and reproduce the same real samples, meaning  $\mathcal{D} \cap \mathcal{D}_{syn} = \emptyset$ . It should be noted that we focus on the task of unconditional data synthesising using LLMs, where  $G$  generates synthetic samples independently of any additional context, i.e., without using explicit prompt text.

#### 3.2 VAE-based Representation Learning

**Feature Encoding:** In standard VAEs, an encoder is typically employed to map input data into a latent space. Given structured text data  $s_i$ , we utilize a learnable Transformer-based pre-trained language model (Vaswani et al., 2017; Devlin et al., 2019; Raffel et al., 2020) to obtain the representation vector  $x_i \in \mathbb{R}^{d \times 2}$ , which can be split into the mean and variance. Using the re-parameterization trick (Kingma and Welling, 2014), we then obtain the latent feature  $z \in \mathbb{R}^d$ :

$$z = \mu + \sigma \odot \epsilon, \quad (1)$$

where  $\mu$  and  $\sigma$  are the mean and standard deviation output by the encoder, and  $\epsilon$  is sampled from a

standard normal distribution  $\mathcal{N}(0, I)$ .

**LLM Decoding:** After generating the latent feature  $z$ , we employ a frozen-parameter LLM to reconstruct the input text  $s$  in a causal language modeling manner. The rationale for freezing the LLM parameters is to avoid retraining and to preserve its general knowledge and reasoning capabilities. Consequently, aligning the two different modalities, whereas the latent space and the LLM input space, presents a significant challenge. To address this, we propose a novel latent feature injector using soft prompting and design a corresponding injector network; specific details are provided in Section 3.4.

**VAE Model Training Objective:** The VAE model is typically trained using the Evidence Lower Bound (ELBO) loss function. Following previous work (Burgess et al., 2018), we adopt the  $\beta$ -VAE training strategy (Higgins et al., 2017), which introduces a weighting parameter  $\beta$  to control the contribution of the KL divergence loss in the total loss function. Specifically, when  $\beta = 0$ , the model reduces to a standard autoencoder. For  $\beta > 0$ , the KL constraint encourages learning a smoother latent space:

$$\text{ELBO}_\beta = L_{\text{rec}} - \beta L_{\text{kl}}, \quad (2)$$

$$L_{\text{rec}} = \mathbb{E}_{q_\phi(z|x)} (\log p_\theta(x|z)), \quad (3)$$

$$L_{\text{kl}} = D_{\text{KL}}(q_\phi(z|x) \parallel p(z)), \quad (4)$$

where  $p_\theta(x|z)$  is the language modeling reconstruction likelihood,  $q_\phi(z|x)$  is the approximate posterior, and  $p(z)$  is the prior over the latent space, i.e., Gaussian distribution. In our model design, considering the denoising network of latent diffusion, we adopt an decreasing  $\beta$  adjustment strategy. We initially set a larger  $\beta$  weight to enforce a strong regularization on the latent space. As the reconstruction loss convergence slows, we decrease the  $\beta$  value to allow the model to focus more on reconstruction accuracy. Additionally, we employ an early stopping mechanism to prevent overfitting.

### 3.3 Latent Space Denoising

Although VAE can learn latent space representations of data, directly sampling from the prior distribution  $p(z)$  often exhibit low quality generated samples. In our preliminary experiments, we observed that directly utilizing the latent features learned by the VAE frequently produces text that is unrelated to the target data distribution. This issue arises due to the discrepancy between the encoder’s learned posterior distribution  $q_\phi(z|x)$  and the prior

$p(z)$ . To address this problem, we introduce a diffusion model in the latent space to more accurately model the true distribution of the latent features. Inspired by Zhang et al. (2024), we extract the latent vectors  $z \in \mathcal{Z}$  from the trained VAE for each data point  $x \in \mathcal{D}_{\text{train}}$ . Starting from the initial latent vector  $z_0$ , we progressively add noise over time following a linear schedule to get  $z_t$ . During the reverse diffusion process, we employ a standard continuous denoising network to recover  $z_0$  (Song et al., 2021). For the training objective, we optimize the diffusion model through denoising score matching (Karras et al., 2022):

$$z_t = z_0 + \sigma(t)\epsilon, \epsilon \in \mathcal{N}(0, I), \quad (5)$$

$$dz_t = -\dot{\sigma}(t)\sigma(t)\nabla_{z_t} \log p(z_t)dt + \sqrt{2\dot{\sigma}(t)\sigma(t)}d\omega_t. \quad (6)$$

In forward process Eq.5,  $z_t$  is the latent variable at time  $t$ , and  $\sigma(t)$  is a time-dependent noise scale function. As for backward process Eq.6,  $\dot{\sigma}(t)$  stands for the time derivative of  $\sigma(t)$ , and  $\nabla_{z_t} \log p(z_t)$  is the gradient of the log probability density with respect to  $z_t$ , also known as the score function, and  $d\omega_t$  is an increment of the Wiener process (standard Brownian motion). As for diffusion model training loss Eq.7,  $\epsilon_\theta(z_t, t)$  is the neural network that predicts the noise  $\epsilon$  given  $z_t$  and  $t$ .

$$\mathcal{L}_{\text{diff}} = \mathbb{E}_{t \sim p(t), z_0 \sim p(z_0), \epsilon \sim \mathcal{N}(0, I)} \|\epsilon_\theta(z_t, t) - \epsilon\|^2, \quad (7)$$

The detailed description for diffusion model could be found in Appendix A.2.

### 3.4 Latent Feature Injection

After constructing a latent space that captures the true data distribution, two challenges remain: 1) *Aligning latent space with LLM’s input space.* How can the decoding LLM process the latent vector  $z$  to steer a powerful language model for realistic data generation? 2) *Seamless Integration with LLM Knowledge:* How can we integrate external information without disrupting the LLM’s internal knowledge? Motivated by adapter training methods in LLM fine-tuning (Lester et al., 2021; Li and Liang, 2021; Houlsby et al., 2019; Liu et al., 2023a), we consider the soft prompt latent injection approach to incorporate  $z$  into LLM decoding without training the model weights. Specifically, after obtaining the latent representation  $z$ , we use an upper MLP to map it into  $k$  soft prompt token embeddings, denoted as  $\mathbf{H}_{\text{latent}} \in \mathbb{R}^{k \times d}$ . These



Table 1: Performance of downstream tasks using generated **tabular** data. We evaluate the quality from: performance in machine learning efficiency (**MLE**) task, and column-wise distribution density estimation ( $\rho$ ) task.  $\uparrow, \downarrow$  indicate that higher (or lower) metrics correspond to better performance. **Boldface** indicates DiffLM surpasses the SoTA model based on language models. **Red Boldface** denotes DiffLM exceeds the performance achieved using real data.

Method	Adult		Default		Magic		Shoppers		Beijing	
	MLE $\uparrow$	$\rho$ $\downarrow$	MLE $\uparrow$	$\rho$ $\downarrow$	MLE $\uparrow$	$\rho$ $\downarrow$	MLE $\uparrow$	$\rho$ $\downarrow$	MLE $\downarrow$	$\rho$ $\downarrow$
Real	0.927	-	0.770	-	0.946	-	0.926	-	0.423	-
SMOTE	0.899	1.60	0.741	1.48	0.934	0.91	0.911	2.68	0.593	1.85
CTGAN	0.886	16.84	0.696	16.83	0.855	9.810	0.875	21.15	0.902	21.39
TVAE	0.878	14.22	0.724	10.17	0.887	8.250	0.871	24.51	0.770	19.16
GOGGLE	0.778	16.97	0.584	17.02	0.654	1.900	0.658	22.33	1.090	16.93
CoDi	0.871	21.38	0.525	15.77	0.932	11.56	0.865	31.84	0.818	16.94
TabSyn	0.915	0.58	0.764	0.85	0.938	0.88	0.920	1.43	0.582	1.12
GPT-4 <sub>ICL</sub>	0.889	32.55	-	-	0.864	10.07	0.835	41.11	0.992	26.1
Mistral-7B <sub>ICL</sub>	0.803	29.22	0.732	36.00	0.881	25.64	0.882	42.00	0.865	12.45
Qwen2.5-14B <sub>ICL</sub>	0.848	17.28	0.737	27.77	0.831	22.72	0.783	52.69	1.289	27.46
GReaT	0.913	12.12	0.755	19.94	0.888	16.16	0.902	14.51	0.653	8.25
DiffLM ( <i>ours</i> )	0.906	<b>9.74</b>	<b>0.794</b>	<b>9.06</b>	<b>0.917</b>	<b>7.53</b>	<b>0.915</b>	<b>10.07</b>	0.696	<b>6.35</b>

soft embeddings serve as a steering vector, which is concatenated before the  $\langle \text{BOS} \rangle$  token to assist the LLM in decoding. The detailed process is illustrated in Figure 4. We also conduct ablation experiments in Section 5 with the other two injection methods proposed by Li et al. (2020), which validated that our methods obtain the best reconstruction loss and downstream task performance.

## 4 Experiments

In this section, we evaluate the generation quality of the DiffLM method on multiple public benchmarks across three tasks: 1) Tabular Data Generation: We compare DiffLM with SoTA tabular generation algorithms, demonstrating its strong capability in structured data generation. 2) Code Generation: DiffLM showcases the ability to integrate structured data priors with its internal knowledge. The results on synthetic data are even better than real ones. 3) Tool Generation: DiffLM can quickly adapt to complex function call scenarios, highlighting its flexibility and adaptability. All experiments adopt Mistral-v0.3 as the frozen VAE decoder. Additional implementation details for reproduction can be found in Appendix B.3.

### 4.1 Tabular Data Generation

**Benchmarking.** We selected five publicly available datasets for evaluation, encompassing both classification and regression tasks: Adult, Beijing,

Default, Magic, and Shoppers. The properties of datasets are presented in Table 5. To assess the quality of synthetic data, we employed two perspectives: 1) **Low-order statistical metrics**, where we quantified column-wise density estimation using the Kolmogorov-Smirnov Test for numerical columns and the Total Variation Distance for categorical columns; 2) **Downstream task performance**, where we measured the predictive accuracy on test data of classifiers or regressors trained on the generated data.

**Baselines.** We selected a comprehensive set of classic and SoTA tabular data generation models with diverse architectures for comparison. First, we consider the performance on real data as the upper bound for evaluation. Secondly, we included the classic method, synthetic minority over-sampling technique (SMOTE) (Chawla et al., 2002), which generates new synthetic data patterns by performing linear interpolation between minority class samples and their  $k$  nearest neighbors. Additionally, for neural network-based tabular generation algorithms, we considered six baselines across different architectures: 1) *GAN*-based models: CTGAN (Xu et al., 2019); 2) *VAE*-based models: TVAE (Xu et al., 2019), GOGGLE (Liu et al., 2023b); 3) *Diffusion*-based models: CoDi (Lee et al., 2023), TabSyn (Zhang et al., 2024); 4) *LLM*-based: 5-shot ICL-based generation, where structural information for each dataset (specifically, col-

Table 2: pass@k scores on **HumanEval** and **MBPP**. We follow [Chen et al. \(2021\)](#) for estimating pass@k, where  $n > k$  solutions are generated per problem with  $p = 0.95$  and a temperature of 0.2 to calculate the success rate with zero-shot learning. **Boldface** indicates that DiffLM surpasses the performance achieved with real data. **Red Boldface** indicates that DiffLM surpasses the base model’s performance.

Model	Size	HumanEval			MBPP		
		pass@1	pass@10	pass@100	pass@1	pass@10	pass@100
GPT-4	-	67.00	-	-	-	-	-
CodeLLaMA	7B	33.50	59.60	85.90	41.40*	66.70*	82.50*
	34B	48.80	76.80	93.00	55.00*	76.20*	86.60*
Mistral-Base	7B	27.79	41.22	56.37	37.31	52.02	59.65
	12B	10.12 <sup>†</sup>	20.91 <sup>†</sup>	28.93 <sup>†</sup>	43.38	61.44	69.09
Mistral-Instruct	7B	36.09	52.95	64.18	38.45	50.77	59.17
	12B	7.08 <sup>†</sup>	12.43 <sup>†</sup>	16.14 <sup>†</sup>	52.20	63.61	69.02
<b>Mistral-Real-Code</b>	7B	28.58	42.24	54.24	27.15	42.21	48.14
	12B	36.97	52.04	60.95	34.79	45.49	50.22
<b>Mistral-DiffLM-Code</b>	7B	<b>35.37</b>	<b>47.36</b>	<b>54.38</b>	<b>32.70</b>	41.65	47.39
	12B	<b>42.24</b>	<b>56.02</b>	<b>61.97</b>	<b>44.42</b>	<b>52.35</b>	<b>55.70</b>

\* These results are evaluated under a 3-shot setting.

<sup>†</sup> The vanilla Mistral-Nemo 12B models fail to pass the HumanEval benchmark, resulting in a lower score. We have conducted multiple evaluations and report the average performance.

umn names and data types for each row) is also provided. We leverage GPT-4, Mistral-v0.3-7B-instruct, and Qwen2.5-14B-instruct models for synthetic data generation. Additionally, we include GReaT ([Borisov et al., 2023](#)), which attempts to fine-tune a GPT-2 ([Radford et al., 2019](#)) for table synthesis. We also report the GReaT result with Mistral model ([Jiang et al., 2023](#)) in Appendix C.6. It is worth noting that we compare with the SoTA generative models not to merely outperform them in tabular generation but to demonstrate that our flexible DiffLM can achieve comparable performance while offering additional advantages.

**Evaluation.** Table 1 presents the quality assessment results of the generated data. For different tabular datasets, we train an XGBoost classifier or regressor on the synthetic data to predict label values, evaluating performance using AUC and RMSE. The results indicate that the performance of the LLM-based synthetic data generation methods leveraging ICL is generally lower; even GPT-4, the best-performing ICL-based model, consistently achieves inferior results across all datasets compared to the fine-tuned GReaT model. However, our proposed DiffLM method consistently outperforms the current LLM-based SoTA GReaT on most datasets. Notably, on the *Default* dataset, the prediction accuracy using DiffLM’s synthetic

data surpasses that obtained by training on real data. This suggests that DiffLM’s approach of integrating the real data distribution with its own learned knowledge can provide richer information for downstream tasks while preserving the original data structure. In other words, the synthetic data generated by DiffLM contains additional knowledge compared to real data, which is challenging to achieve with previous methods. Moreover, our generated results achieve performance comparable to prior methods in column-wise distribution density estimation. Although the TabSyn method attains superior performance on several datasets, it should be noted that our approach focuses on general, plug-gable generation control for large language model, rather than training data synthesis models from scratch for specific domains. Despite this, in tabular data generation, our method’s performance is on par with these domain-specific methods.

## 4.2 Code Generation

**Benchmarking.** In the code generation scenario, to simplify the problem, we focus on Python code and use the Flytech<sup>1</sup> dataset as real data, which contains 24,813 unique real user queries and the corresponding Python code fulfilling those requests.

<sup>1</sup><https://huggingface.co/datasets/flytech/python-codes-25k>

We discard the user queries and use only the code to train DiffLM. After generating synthetic code data, we continue pre-training the Mistral 7B v0.3 base model (Jiang et al., 2023) using a smaller learning rate, i.e.,  $1e-5$ , in a causal language modeling objective. We then benchmark the trained model on code generation tasks, selecting two mainstream benchmarks: HumanEval (Chen et al., 2021) and MBPP (Austin et al., 2021b). To better understand the performance changes of the base model, we also experiment larger models like Mistral Nemo with 12B parameters.

**Baselines.** We include the performance from recent code LLMs. First, we consider the CodeL-LaMA (Rozière et al., 2023) series, which use approximately 600B tokens to continue pre-training the LLaMA-2 (Touvron et al., 2023) base model, injecting strong code capabilities through multi-task learning. Additionally, we compare with the Mistral base model (Jiang et al., 2023) and its instruction-tuned variants, the latter could representing the upper bound of code capabilities for this architecture.

**Evaluation.** We report the code generation capabilities in Table 2. Specifically, Mistral-Real-Code and Mistral-DiffLM-Code denote models that were further pre-trained on real data and synthetic data generated by DiffLM, respectively. The 7B models are based on Mistral-0.3-Base, and the 12B models are based on Mistral-Nemo-Base. Both models were trained for 3 epochs on the same amount of data using identical hyperparameters, effectively serving as a controlled experiment where the data source is the only variable. The results indicate that simply continuing to pre-train the Mistral model with a small amount of code data leads to inconsistent impacts on code generation capabilities. Specifically, Mistral-Real-Code shows a slight improvement on *HumanEval* but a significant decline on *MBPP*. However, using our synthetic data to continue pre-training the base model yields better results than using real data. For instance, Mistral-DiffLM-Code-7B, achieved a 7% improvement over the base model, even outperforming the Code Llama 7B model that was trained with more extensive data. In summary, in the code generation scenario, we focus on the differing impacts of real data and synthetic data, further demonstrating that DiffLM can generate synthetic data that is even more effective than real data in enhancing downstream task performance.

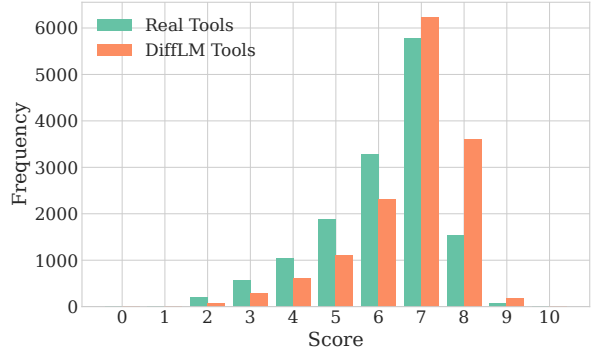


Figure 2: GPT-4 evaluation scores for tools from the ToolBench dataset and tools generated by DiffLM. The evaluation prompt considers aspects such as clarity, specificity, completeness, consistency, and applicability.

Table 3: Win rate of DiffLM generated data. GPT-4 performs preference scoring on all real tools and synthetic tools within the same category, considering aspects like comprehensiveness and diversity.

	Rate %
DiffLM Win	28.3
Equal	6.8
Real Win	64.9

### 4.3 Tool Generation

**Evaluation.** To address more complex structured data generation scenarios, we further conduct a tool synthesis task. Specifically, we select the ToolBench (Qin et al., 2024) dataset as a benchmark for comparison, which is constructed based on the RapidAPI<sup>2</sup> platform by crawling APIs created by real users and synthesizing related dialogue SFT data using GPT<sup>3</sup>. We use its toolset to train DiffLM and then sample an equal number of tools for comparison. We assess the usability of the generated tools from two perspectives: 1) **Single-Tool Quality:** We use GPT-4 as an annotator to score the real and synthetic data across multiple dimensions on a scale from 0 to 10, where the results are illustrated in Figure 2. 2) **Category-Level Preference:** We collect all tools within the same category and use GPT-4 to perform preference scoring between real tools and synthetic tools, as presented in Table 3. The specific evaluation prompts are provided in the appendix B.2. From the results, DiffLM’s synthetic data achieves higher scores in the single-tool scoring task, indicating that leveraging the internal knowledge and generative capabilities of LLMs

<sup>2</sup><https://rapidapi.com/hub>

<sup>3</sup><https://chat.openai.com>

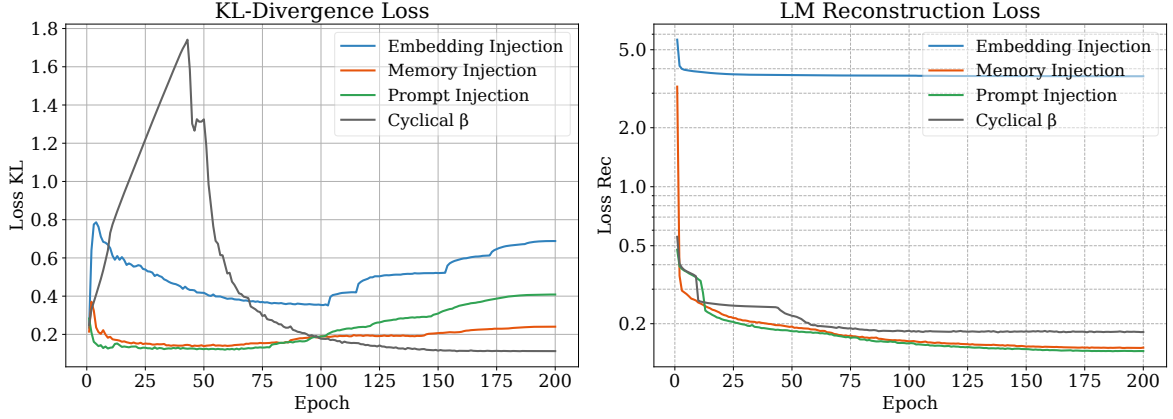


Figure 3: Model loss curves under different latent feature injection methods and different  $\beta$  adjustment strategies. The left is the KL-divergence loss trends, and the right is the language modeling reconstruction loss on a logarithmic scale. In the cyclical  $\beta$  strategy,  $\beta$  increases linearly from 0 to 0.2. The other methods employ a decreasing  $\beta$ , starting from a maximum value of 0.1 and decreasing to a minimum of 0.001.

allows us to create tool descriptions and input/output parameter definitions of higher textual quality. Additionally, in the category-level preference evaluation, nearly 1/3 of the tool types surpass or are on par with real data in terms of diversity and usability. Since DiffLM can sample and generate tools indefinitely to increase coverage, we believe there is room for further improvement in this metric.

## 5 Analysis

**The effect of adaptive  $\beta$  adjustment.** As described in Section 3.2, we use a decreasing  $\beta$  adjustment strategy to train the VAE latent space. Here, we compare this with another method that uses a cyclical schedule to anneal  $\beta$  (Fu et al., 2019), evaluating both the loss decline curves and downstream task performance to demonstrate the effectiveness of our decreasing strategy. Firstly, as shown in Figure 3, the KL-divergence loss trends under decreasing  $\beta$  exhibit a pattern where the loss first increases, then decreases, and then increases again. This indicates that during the early stages of VAE training, DiffLM uses a larger  $\beta$  to focus on the divergence between the embedding distribution and the standard Gaussian. This helps quickly learn a standard latent space to stabilize the training of the LLM module. Subsequently, when the reconstruction loss reaches a bottleneck, it gradually reduces the weight of the KL-divergence loss. At this point, the training objective shifts towards obtaining a decoder with stronger generative capabilities. As a result, the KL loss gradually increases and eventually stabilizes at a fairly low value. From the results, our decreasing  $\beta$  method achieves the lowest

Table 4: The results of MLE and  $\rho$  under different latent feature injections and  $\beta$  adjustments on *Adult* dataset.

Models	MLE $\uparrow$	$\rho$ $\downarrow$
DiffLM-Cycle $\beta$	0.872	16.79
DiffLM-Embed	-	-
DiffLM-Memory	0.875	17.05
DiffLM-Prompt	<b>0.906</b>	<b>9.74</b>

reconstruction loss. Additionally, by introducing the latent diffusion process, we address the issue of distribution discrepancy. Therefore, as shown in Table 4, compared to the cyclical method, the decreasing  $\beta$  strategy used in this paper results in stronger generative ability.

**The effect of latent feature injection.** We also compare our proposed soft prompt latent feature injection method with previously explored methods such as KV memory injection and input embedding injection (Li et al., 2020); implementation details are illustrated in Figure 4. Specifically, the loss convergence on the validation dataset for different injection methods are shown in Figure 3. The input embedding method leads to suboptimal training results, where the reconstruction loss ceases to decrease after reaching around 3.6. This indicates that such a simple injection method struggles to effectively convey complex real distribution information to the LLM decoder. Meanwhile, the soft prompt method slightly outperforms KV memory in terms of reconstruction loss. However, as shown in Table 4, on downstream task performance using the *Adult* dataset, our proposed soft prompt approach



achieves higher (2%) classification accuracy and better column density.

## 6 Conclusion

In this paper, we propose DiffLM, a novel framework that enhances LLMs’ ability to generate high-quality synthetic data by integrating real-world data distributions. DiffLM maps real data into a latent space via VAE, which is then injected into LLM decoding through a causal language modeling objective. A diffusion process further refines the latent distribution, reducing sampling discrepancies. To ensure flexible and non-intrusive control over data quality and structure, DiffLM freezes LLM parameters and employs latent features as plug-in modules. Experiments show that DiffLM generates consistent data, enabling downstream models to match or even exceed the performance of those trained on real data. For future research, our work could help build data flywheels for LLM applications and facilitate dataset curation for low-resource domains.

## Limitations

Our work, while offering valuable contributions to synthetic data generation, has several limitations. First, our approach focuses primarily on structured data synthesis, such as tabular data generation, code generation, and tool generation. It does not address the generation of more subjective or nuanced data, such as sentiment-specific data or tasks requiring varied levels of complexity or capability. Additionally, our decoupling of data distribution learning may need further refinement to accommodate such subjective text synthesis tasks. Second, due to time and hardware constraints, we limited our study to a relatively simple VAE and diffusion network, and used LLMs up to 7B parameters for decoding. Future research could explore the potential of scaling these models further, using even larger architectures to better evaluate and validate the effectiveness of the DiffLM framework in data synthesis tasks.

## Acknowledgments

This work is supported by the National Natural Science Foundation of China (62272439) and the Fundamental Research Funds for the Central Universities, and is conducted during Ying Zhou’s internship at ByteDance Inc.

## References

- Mohammad Hossein Amani, Nicolas Mario Baldwin, Amin Mansouri, Martin Josifoski, Maxime Peyrard, and Robert West. 2024. Symbolic autoencoding for self-supervised sequence learning. *CoRR*, abs/2402.10575.
- Ateret Anaby-Tavor, Boaz Carmeli, Esther Goldbraich, Amir Kantor, George Kour, Segev Shlomov, Naama Tepper, and Naama Zwerdling. 2020. Do not have enough data? deep learning to the rescue! In *AAAI*, pages 7383–7390. AAAI Press.
- Jacob Austin, Daniel D. Johnson, Jonathan Ho, Daniel Tarlow, and Rianne van den Berg. 2021a. Structured denoising diffusion models in discrete state-spaces. In *NeurIPS*, pages 17981–17993.
- Jacob Austin, Augustus Odena, Maxwell I. Nye, Maarten Bosma, Henryk Michalewski, David Dohan, Ellen Jiang, Carrie J. Cai, Michael Terry, Quoc V. Le, and Charles Sutton. 2021b. Program synthesis with large language models. *CoRR*, abs/2108.07732.
- André Bauer, Simon Trapp, Michael Stenger, Robert Leppich, Samuel Kounev, Mark Leznik, Kyle Chard, and Ian T. Foster. 2024. Comprehensive exploration of synthetic data generation: A survey. *CoRR*, abs/2401.02524.
- James Betker, Gabriel Goh, Li Jing, Tim Brooks, Jianfeng Wang, Linjie Li, Long Ouyang, Juntang Zhuang, Joyce Lee, Yufei Guo, et al. 2023. Improving image generation with better captions. *Computer Science*. <https://cdn.openai.com/papers/dall-e-3.pdf>, 2(3):8.
- Vadim Borisov, Kathrin Seßler, Tobias Leemann, Martin Pawelczyk, and Gjergji Kasneci. 2023. Language models are realistic tabular data generators. In *ICLR*. OpenReview.net.
- Samuel R. Bowman, Luke Vilnis, Oriol Vinyals, Andrew M. Dai, Rafal Józefowicz, and Samy Bengio. 2016. Generating sentences from a continuous space. In *CoNLL*, pages 10–21. ACL.
- Christopher P. Burgess, Irina Higgins, Arka Pal, Loïc Matthey, Nick Watters, Guillaume Desjardins, and Alexander Lerchner. 2018. Understanding disentangling in  $\beta$ -vae. *CoRR*, abs/1804.03599.
- Nitesh V. Chawla, Kevin W. Bowyer, Lawrence O. Hall, and W. Philip Kegelmeyer. 2002. SMOTE: synthetic minority over-sampling technique. *J. Artif. Intell. Res.*, 16:321–357.
- Jiaao Chen, Aston Zhang, Mu Li, Alex Smola, and Diyi Yang. 2023. A cheaper and better diffusion language model with soft-masked noise. In *EMNLP*, pages 4765–4775. Association for Computational Linguistics.
- Mark Chen, Jerry Tworek, Heewoo Jun, Qiming Yuan, Henrique Pondé de Oliveira Pinto, Jared Kaplan, Harri Edwards, Yuri Burda, and et al. 2021. Evaluating large language models trained on code. *CoRR*, abs/2107.03374.

- Jasper Dekoninck, Marc Fischer, Luca Beurer-Kellner, and Martin T. Vechev. 2024. Controlled text generation via language model arithmetic. In *ICLR*. OpenReview.net.
- Jacob Devlin, Ming-Wei Chang, Kenton Lee, and Kristina Toutanova. 2019. BERT: pre-training of deep bidirectional transformers for language understanding. In *NAACL-HLT (1)*, pages 4171–4186. Association for Computational Linguistics.
- Tuan Dinh, Yuchen Zeng, Ruisu Zhang, Ziqian Lin, Michael Gira, Shashank Rajput, Jy-yong Sohn, Dimitris S. Papailiopoulos, and Kangwook Lee. 2022. LIFT: language-interfaced fine-tuning for non-language machine learning tasks. In *NeurIPS*.
- Hao Fu, Chunyuan Li, Xiaodong Liu, Jianfeng Gao, Asli Celikyilmaz, and Lawrence Carin. 2019. Cyclical annealing schedule: A simple approach to mitigating KL vanishing. In *NAACL-HLT (1)*, pages 240–250. Association for Computational Linguistics.
- Shansan Gong, Mukai Li, Jiangtao Feng, Zhiyong Wu, and Lingpeng Kong. 2023. Diffuseq: Sequence to sequence text generation with diffusion models. In *ICLR*. OpenReview.net.
- Shuyang Gu, Dong Chen, Jianmin Bao, Fang Wen, Bo Zhang, Dongdong Chen, Lu Yuan, and Baining Guo. 2022. Vector quantized diffusion model for text-to-image synthesis. In *CVPR*, pages 10686–10696. IEEE.
- Yuxuan Gu, Xiaocheng Feng, Sicheng Ma, Lingyuan Zhang, Heng Gong, Weihong Zhong, and Bing Qin. 2023. Controllable text generation via probability density estimation in the latent space. In *ACL (1)*, pages 12590–12616. Association for Computational Linguistics.
- Ishaan Gulrajani, Kundan Kumar, Faruk Ahmed, Adrien Ali Taïga, Francesco Visin, David Vázquez, and Aaron C. Courville. 2017. Pixelvae: A latent variable model for natural images. In *ICLR (Poster)*. OpenReview.net.
- Serhii Havrylov and Ivan Titov. 2020. Preventing posterior collapse with levenshtein variational autoencoder. *CoRR*, abs/2004.14758.
- Zhengfu He, Tianxiang Sun, Qiong Tang, Kuanning Wang, Xuanjing Huang, and Xipeng Qiu. 2023. Diffusionbert: Improving generative masked language models with diffusion models. In *ACL (1)*, pages 4521–4534. Association for Computational Linguistics.
- Irina Higgins, Loïc Matthey, Arka Pal, Christopher P. Burgess, Xavier Glorot, Matthew M. Botvinick, Shakir Mohamed, and Alexander Lerchner. 2017. beta-vae: Learning basic visual concepts with a constrained variational framework. In *ICLR (Poster)*. OpenReview.net.
- Neil Houlsby, Andrei Giurgiu, Stanislaw Jastrzebski, Bruna Morrone, Quentin de Laroussilhe, Andrea Gesmundo, Mona Attariyan, and Sylvain Gelly. 2019. Parameter-efficient transfer learning for NLP. In *ICML*, volume 97 of *Proceedings of Machine Learning Research*, pages 2790–2799. PMLR.
- Albert Q. Jiang, Alexandre Sablayrolles, Arthur Mensch, Chris Bamford, Devendra Singh Chaplot, Diego de Las Casas, Florian Bressand, Gianna Lengyel, and et al. 2023. Mistral 7b. *CoRR*, abs/2310.06825.
- Martin Josifoski, Marija Sakota, Maxime Peyrard, and Robert West. 2023. Exploiting asymmetry for synthetic training data generation: Synthie and the case of information extraction. In *EMNLP*, pages 1555–1574. Association for Computational Linguistics.
- Lukasz Kaiser and Samy Bengio. 2018. Discrete autoencoders for sequence models. *CoRR*, abs/1801.09797.
- Tero Karras, Miika Aittala, Timo Aila, and Samuli Laine. 2022. Elucidating the design space of diffusion-based generative models. In *NeurIPS*.
- Nitish Shirish Keskar, Bryan McCann, Lav R. Varshney, Caiming Xiong, and Richard Socher. 2019. CTRL: A conditional transformer language model for controllable generation. *CoRR*, abs/1909.05858.
- Diederik P. Kingma and Max Welling. 2014. Auto-encoding variational bayes. In *ICLR*.
- Varun Kumar, Ashutosh Choudhary, and Eunah Cho. 2020. Data augmentation using pre-trained transformer models. *CoRR*, abs/2003.02245.
- Chaejeong Lee, Jayoung Kim, and Noseong Park. 2023. Codi: Co-evolving contrastive diffusion models for mixed-type tabular synthesis. In *ICML*, volume 202 of *Proceedings of Machine Learning Research*, pages 18940–18956. PMLR.
- Brian Lester, Rami Al-Rfou, and Noah Constant. 2021. The power of scale for parameter-efficient prompt tuning. In *EMNLP (1)*, pages 3045–3059. Association for Computational Linguistics.
- Chunyuan Li, Xiang Gao, Yuan Li, Baolin Peng, Xiujuan Li, Yizhe Zhang, and Jianfeng Gao. 2020. Optimus: Organizing sentences via pre-trained modeling of a latent space. In *EMNLP (1)*, pages 4678–4699. Association for Computational Linguistics.
- Xiang Lisa Li and Percy Liang. 2021. Prefix-tuning: Optimizing continuous prompts for generation. In *ACL/IJCNLP (1)*, pages 4582–4597. Association for Computational Linguistics.
- Xiang Lisa Li, John Thickstun, Ishaan Gulrajani, Percy Liang, and Tatsunori B. Hashimoto. 2022. Diffusion-lm improves controllable text generation. In *NeurIPS*.

- Zhuoyan Li, Hangxiao Zhu, Zhuoran Lu, and Ming Yin. 2023. Synthetic data generation with large language models for text classification: Potential and limitations. In *EMNLP*, pages 10443–10461. Association for Computational Linguistics.
- Zhenghao Lin, Yeyun Gong, Yelong Shen, Tong Wu, Zhihao Fan, Chen Lin, Nan Duan, and Weizhu Chen. 2023. Text generation with diffusion language models: A pre-training approach with continuous paragraph denoise. In *ICML*, volume 202 of *Proceedings of Machine Learning Research*, pages 21051–21064. PMLR.
- Haotian Liu, Chunyuan Li, Qingyang Wu, and Yong Jae Lee. 2023a. Visual instruction tuning. In *NeurIPS*.
- Tennison Liu, Zhaozhi Qian, Jeroen Berrevoets, and Mihaela van der Schaar. 2023b. GOGGLE: generative modelling for tabular data by learning relational structure. In *ICLR*. OpenReview.net.
- Lin Long, Rui Wang, Ruixuan Xiao, Junbo Zhao, Xiao Ding, Gang Chen, and Haobo Wang. 2024. On llms-driven synthetic data generation, curation, and evaluation: A survey. In *ACL (Findings)*, pages 11065–11082. Association for Computational Linguistics.
- Simian Luo, Yiqin Tan, Longbo Huang, Jian Li, and Hang Zhao. 2023a. Latent consistency models: Synthesizing high-resolution images with few-step inference. *CoRR*, abs/2310.04378.
- Yun Luo, Zhen Yang, Fandong Meng, Yafu Li, Jie Zhou, and Yue Zhang. 2023b. An empirical study of catastrophic forgetting in large language models during continual fine-tuning. *CoRR*, abs/2308.08747.
- Raul Puri, Ryan Spring, Mohammad Shoeybi, Mostofa Patwary, and Bryan Catanzaro. 2020. Training question answering models from synthetic data. In *EMNLP (1)*, pages 5811–5826. Association for Computational Linguistics.
- Yujia Qin, Shihao Liang, Yining Ye, Kunlun Zhu, Lan Yan, Yaxi Lu, Yankai Lin, Xin Cong, Xiangru Tang, Bill Qian, Sihan Zhao, Lauren Hong, Runchu Tian, Ruobing Xie, Jie Zhou, Mark Gerstein, Dahai Li, Zhiyuan Liu, and Maosong Sun. 2024. Toolllm: Facilitating large language models to master 16000+ real-world apis. In *ICLR*. OpenReview.net.
- Alec Radford, Jeff Wu, Rewon Child, David Luan, Dario Amodei, and Ilya Sutskever. 2019. Language models are unsupervised multitask learners.
- Colin Raffel, Noam Shazeer, Adam Roberts, Katherine Lee, Sharan Narang, Michael Matena, Yanqi Zhou, Wei Li, and Peter J. Liu. 2020. Exploring the limits of transfer learning with a unified text-to-text transformer. *J. Mach. Learn. Res.*, 21:140:1–140:67.
- Machel Reid, Vincent Josua Hellendoorn, and Graham Neubig. 2023. Diffuser: Diffusion via edit-based reconstruction. In *ICLR*. OpenReview.net.
- Robin Rombach, Andreas Blattmann, Dominik Lorenz, Patrick Esser, and Björn Ommer. 2022. High-resolution image synthesis with latent diffusion models. In *CVPR*, pages 10674–10685. IEEE.
- Baptiste Rozière, Jonas Gehring, Fabian Gloeckle, Sten Sootla, Itai Gat, Xiaoqing Ellen Tan, Yossi Adi, Jingyu Liu, and et al. 2023. Code llama: Open foundation models for code. *CoRR*, abs/2308.12950.
- Yang Song, Jascha Sohl-Dickstein, Diederik P. Kingma, Abhishek Kumar, Stefano Ermon, and Ben Poole. 2021. Score-based generative modeling through stochastic differential equations. In *ICLR*. OpenReview.net.
- Ruixiang Tang, Xiaotian Han, Xiaoqian Jiang, and Xia Hu. 2023. Does synthetic data generation of llms help clinical text mining? *CoRR*, abs/2303.04360.
- Hugo Touvron, Louis Martin, Kevin Stone, Peter Albert, Amjad Almahairi, Yasmine Babaei, Nikolay Bashlykov, Soumya Batra, and et al. 2023. Llama 2: Open foundation and fine-tuned chat models. *CoRR*, abs/2307.09288.
- Ashish Vaswani, Noam Shazeer, Niki Parmar, Jakob Uszkoreit, Llion Jones, Aidan N. Gomez, Lukasz Kaiser, and Illia Polosukhin. 2017. Attention is all you need. In *NIPS*, pages 5998–6008.
- Veniamin Veselovsky, Manoel Horta Ribeiro, Akhil Arora, Martin Josifoski, Ashton Anderson, and Robert West. 2023. Generating faithful synthetic data with large language models: A case study in computational social science. *CoRR*, abs/2305.15041.
- Jerry Wei, Chengrun Yang, Xinying Song, Yifeng Lu, Nathan Hu, Dustin Tran, Daiyi Peng, Ruibo Liu, Da Huang, Cosmo Du, and Quoc V. Le. 2024. Long-form factuality in large language models. *CoRR*, abs/2403.18802.
- Siyuan Wu, Yue Huang, Chujie Gao, Dongping Chen, Qihui Zhang, Yao Wan, Tianyi Zhou, Xiangliang Zhang, Jianfeng Gao, Chaowei Xiao, and Lichao Sun. 2024. Unigen: A unified framework for textual dataset generation using large language models. *CoRR*, abs/2406.18966.
- Lei Xu, Maria Skoularidou, Alfredo Cuesta-Infante, and Kalyan Veeramachaneni. 2019. Modeling tabular data using conditional GAN. In *NeurIPS*, pages 7333–7343.
- Shengzhe Xu, Cho-Ting Lee, Mandar Sharma, Raquib Bin Yousuf, Nikhil Muralidhar, and Naren Ramakrishnan. 2024. Are llms naturally good at synthetic tabular data generation? *CoRR*, abs/2406.14541.
- Kevin Yang and Dan Klein. 2021. FUDGE: controlled text generation with future discriminators. In *NAACL-HLT*, pages 3511–3535. Association for Computational Linguistics.

- Jiacheng Ye, Jiahui Gao, Qintong Li, Hang Xu, Jiangtao Feng, Zhiyong Wu, Tao Yu, and Lingpeng Kong. 2022a. Zerogen: Efficient zero-shot learning via dataset generation. In *EMNLP*, pages 11653–11669. Association for Computational Linguistics.
- Jiacheng Ye, Jiahui Gao, Zhiyong Wu, Jiangtao Feng, Tao Yu, and Lingpeng Kong. 2022b. Progen: Progressive zero-shot dataset generation via in-context feedback. In *EMNLP (Findings)*, pages 3671–3683. Association for Computational Linguistics.
- Jiahui Yu, Yuanzhong Xu, Jing Yu Koh, Thang Luong, Gunjan Baid, Zirui Wang, Vijay Vasudevan, Alexander Ku, Yinfei Yang, Burcu Karagol Ayan, Ben Hutchinson, Wei Han, Zarana Parekh, Xin Li, Han Zhang, Jason Baldridge, and Yonghui Wu. 2022a. Scaling autoregressive models for content-rich text-to-image generation. *Trans. Mach. Learn. Res.*, 2022.
- Peiyu Yu, Sirui Xie, Xiaojian Ma, Baoxiong Jia, Bo Pang, Ruiqi Gao, Yixin Zhu, Song-Chun Zhu, and Ying Nian Wu. 2022b. Latent diffusion energy-based model for interpretable text modeling. *CoRR*, abs/2206.05895.
- Yue Yu, Yuchen Zhuang, Jieyu Zhang, Yu Meng, Alexander J. Ratner, Ranjay Krishna, Jiaming Shen, and Chao Zhang. 2023. Large language model as attributed training data generator: A tale of diversity and bias. In *NeurIPS*.
- Hongyi Yuan, Zheng Yuan, Chuanqi Tan, Fei Huang, and Songfang Huang. 2024. Text diffusion model with encoder-decoder transformers for sequence-to-sequence generation. In *NAACL-HLT*, pages 22–39. Association for Computational Linguistics.
- Haopeng Zhang, Xiao Liu, and Jiawei Zhang. 2023. Diffusum: Generation enhanced extractive summarization with diffusion. In *ACL (Findings)*, pages 13089–13100. Association for Computational Linguistics.
- Hengrui Zhang, Jiani Zhang, Zhengyuan Shen, Balasubramaniam Srinivasan, Xiao Qin, Christos Faloutsos, Huzefa Rangwala, and George Karypis. 2024. Mixed-type tabular data synthesis with score-based diffusion in latent space. In *ICLR*. OpenReview.net.



## A Details on Model Design

### A.1 Controllability

We define the controllability of text data synthesis as the ability to generate text that satisfies desired requirements (e.g., structure, topics, domains) (Keskar et al., 2019; Li et al., 2022). Existing methods for structured textual data synthesis often struggle with controllability. On one hand, LLM prompt-based methods relying on prompt engineering or few-shot inference cannot guarantee the diversity and scalability of synthetic data, even with complex human-crafted processes (Long et al., 2024). On the other hand, controlling a LM by fine-tuning it with supervised data (SFT, RLHF) is not only expensive but might also degrade the LLM’s general capability (Keskar et al., 2019; Borisov et al., 2023). Our method addresses these challenges through sampling in the latent space while maintaining data structure due to LLM’s instruction-following ability.

### A.2 Diffusion Process

In this section, we will introduce the general process of latent diffusion models. Latent Diffusion Models (LDMs) are a class of diffusion probabilistic models that operate in the latent space of an autoencoder rather than directly on the high-dimensional data space. By performing diffusion in a compressed latent representation, LDMs significantly reduce computational complexity while maintaining high fidelity in data generation. An LDM consists of two primary components:

1. Autoencoder: Encodes input data  $\mathbf{x}_0$  into a latent representation  $\mathbf{z}_0 = E(\mathbf{x}_0)$  and decodes latent variables back to data space  $\hat{\mathbf{x}} = D(\mathbf{z})$ .
2. Diffusion Model: Defines a diffusion process on the latent variables  $\{\mathbf{z}_t\}_{t=0}^T$ .

It should be noted that the variable used here is independent with main text.

**Forward Process (Diffusion).** The forward diffusion process in latent space progressively adds Gaussian noise to the latent representation over  $T$  timesteps. Starting from the initial latent code  $\mathbf{z}_0 = E(\mathbf{x}_0)$ , obtained by encoding the data  $\mathbf{x}_0$ , the forward process is defined as:

$$q(\mathbf{z}_t | \mathbf{z}_{t-1}) = \mathcal{N}(\mathbf{z}_t; \sqrt{1 - \beta_t} \mathbf{z}_{t-1}, \beta_t \mathbf{I}), \quad (8)$$

where  $\beta_t \in (0, 1)$  is a predefined variance schedule that controls the amount of noise added at each

step  $t$ , and  $\mathcal{N}$  denotes a Gaussian distribution. By recursively applying this process, we can express  $\mathbf{z}_t$  directly in terms of  $\mathbf{z}_0$ :

$$q(\mathbf{z}_t | \mathbf{z}_0) = \mathcal{N}(\mathbf{z}_t; \sqrt{\bar{\alpha}_t} \mathbf{z}_0, (1 - \bar{\alpha}_t) \mathbf{I}), \quad (9)$$

where  $\alpha_t = 1 - \beta_t$  and  $\bar{\alpha}_t = \prod_{s=1}^t \alpha_s$ . This formulation allows efficient sampling of  $\mathbf{z}_t$  at any arbitrary timestep  $t$  without iterating through all previous steps. In this paper, we adopt the Variance Exploding defined perturbation kernels, whereas setting  $s_t = \sqrt{1 - \beta_t}$  and  $\sigma_t = \sqrt{\frac{\beta_t}{1 - \beta_t}}$ . Also, we set  $s_t = 1$  to directly add noise to the data rather than weighted mixing, convert Eq.9 to:

$$q(\mathbf{z}_t | \mathbf{z}_0) = \mathcal{N}(\mathbf{z}_t; \mathbf{0}, \sigma_t^2 \mathbf{I}) \quad (10)$$

**Reverse Process (Denoising).** The reverse diffusion process aims to recover  $\mathbf{z}_0$  from a noisy latent variable  $\mathbf{z}_t \sim \mathcal{N}(0, \mathbf{I})$ . It is parameterized by a neural network  $\epsilon_\theta$ , which predicts the noise component at each timestep:

$$p_\theta(\mathbf{z}_{t-1} | \mathbf{z}_t) = \mathcal{N}(\mathbf{z}_{t-1}; \mu_\theta(\mathbf{z}_t, t), \Sigma_\theta(\mathbf{z}_t, t)). \quad (11)$$

Typically, the model predicts the mean  $\mu_\theta$  while the covariance  $\Sigma_\theta$  is fixed or simplified. By leveraging the properties of the forward process, the mean can be parameterized to predict the original noise  $\epsilon$  added during the forward diffusion:

$$\mu_\theta(\mathbf{z}_t, t) = \frac{1}{\sqrt{\alpha_t}} \left( \mathbf{z}_t - \frac{\beta_t}{\sqrt{1 - \bar{\alpha}_t}} \epsilon_\theta(\mathbf{z}_t, t) \right). \quad (12)$$

This formulation enables the model to denoise  $\mathbf{z}_t$  step by step, ultimately reconstructing  $\mathbf{z}_0$ .

**Learning Objective.** The training objective for LDMs focuses on minimizing the difference between the true noise  $\epsilon$  added during the forward process and the noise predicted by the model  $\epsilon_\theta$ . The simplified loss function is:

$$\mathcal{L}_{\text{latent}} = \mathbb{E}_{\mathbf{x}_0, \epsilon, t} \left[ \|\epsilon - \epsilon_\theta(\mathbf{z}_t, t)\|^2 \right], \quad (13)$$

where  $\mathbf{z}_t$  is sampled as:

$$\mathbf{z}_t = \sqrt{\bar{\alpha}_t} \mathbf{z}_0 + \sqrt{1 - \bar{\alpha}_t} \epsilon, \quad \epsilon \sim \mathcal{N}(0, \mathbf{I}). \quad (14)$$

This objective encourages the model to learn the conditional distribution  $p_\theta(\mathbf{z}_{t-1} | \mathbf{z}_t)$  by accurately predicting the noise component at each timestep.

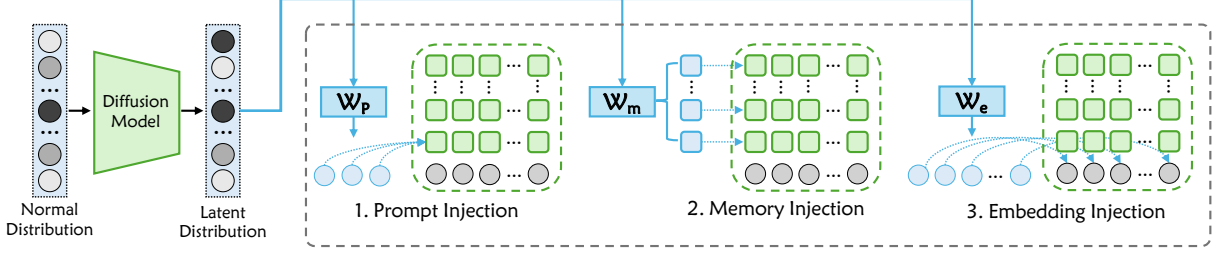


Figure 4: Final data synthesis process. The comparison of different latent feature injection methods is shown in grey dashed box. *Memory Injection* introduces the latent features as past key-value (KV) memories into each attention layer of the LLM. *Embedding Injection* directly adds the latent features to the token embeddings.

**Noise Scheduling.** The noise schedule  $\{\beta_t\}_{t=1}^T$  plays a critical role in the diffusion process. It dictates how quickly noise is added in the forward process and, consequently, affects the difficulty of the reverse denoising task. Common strategies for setting  $\beta_t$  include linear, cosine, and quadratic schedules. We use linear noise schedule, i.e., the perturbation kernel  $\sigma(t) = t$ . As it is an effective schedule, ensuring that the data is sufficiently diffused by timestep  $t$ , while still allowing the model to learn meaningful reverse transitions.

## B Details on Experimental Setup

### B.1 Tabular Data Generation

Table 5 shows the detail information of tabular dataset we use in paper.

### B.2 Tool Judgement Prompts

We present the evaluation prompts used for assessing tool generation quality in Figure 7 and Figure 8.

### B.3 Instructions for Reproduction

In this section, we present the experimental details of DiffLM, including data preprocessing, training hyperparameter settings, and data post-processing filtering methods.

**Data Preprocessing.** Real-world NLP datasets often exhibit inherent structures, such as the context, question, and answer in machine reading comprehension tasks, or key-value pairs in tabular generation tasks. In DiffLM, we convert all structured data into JSON format. For instance, tabular data in a CSV file is transformed into lines of JSON, and tools from ToolBench are abstracted into JSON structures comprising `tool_name`, `tool_description`, `api_name`, and `api_description`. For code data, we use the raw code directly without any preprocessing as input for DiffLM training.

### Hyperparameter Settings.

- VAE Encoder: bert-base-uncased
- VAE Decoder: mistralai/Mistral-7B-Instruct-v0.3
- Soft Prompt Tokens  $k$ : 64
- Soft Prompt Embedding Dimension  $d$ : 4096
- $\beta_{\max} = 0.1$
- $\beta_{\min} = 0.001$
- Diffusion Noise Dimension: 4096

**Generation Filtering.** For inputs in JSON format, we employ column names to filter the generated outputs. A generated result is considered valid only if it contains all required columns. For code generation tasks involving plain text, we do not apply any filtering. We utilize the same filtering criteria across all baseline models.

### B.4 Training Parameters for Baselines.

We reproduced the tabular results using the code released by the original paper, ensuring that all hyperparameters and settings were consistent with the original implementation. All results were almost identical to those reported in the TabSyn paper; therefore, we used the results reported in TabSyn in Table 1 to ensure a fair comparison.

## C Addition Experiment Results

### C.1 Training Data Plagiarism

Data copying is a significant challenge for overfitted generative models in practical applications. To verify that the data generated by DiffLM is not merely copied from the training data, we compute the Distance to Closest Record (DCR) metric. Specifically, for each row in the tabular data, we represent the categorical columns using one-hot vectors and perform min-max normalization on the numerical columns. We then define DCR as

Table 5: Details of tabular dataset. For each dataset, #Num stands for the number of numerical columns, and #Cat stands for the number of categorical columns.

Datasets	#Num	#Cat	#Train	#Validation	#Test	Downstream Task
Adult <sup>1</sup>	6	9	29,304	3,257	16,281	Binary Classification
Beijing <sup>2</sup>	7	5	35,059	4,382	4,383	Binary Classification
Default <sup>3</sup>	14	11	24,000	3,000	3,000	Binary Classification
Magic <sup>4</sup>	10	1	15,216	1,902	1,902	Binary Classification
Shoppers <sup>5</sup>	10	8	9,864	1,233	1,233	Regression

<sup>1</sup> <https://archive.ics.uci.edu/dataset/2/adult>

<sup>2</sup> <https://archive.ics.uci.edu/dataset/381/beijing+pm2+5+data>

<sup>3</sup> <https://archive.ics.uci.edu/dataset/350/default+of+credit+card+clients>

<sup>4</sup> <https://archive.ics.uci.edu/dataset/159/magic+gamma+telescope>

<sup>5</sup> <https://archive.ics.uci.edu/dataset/468/online+shoppers+purchasing+intention+dataset>

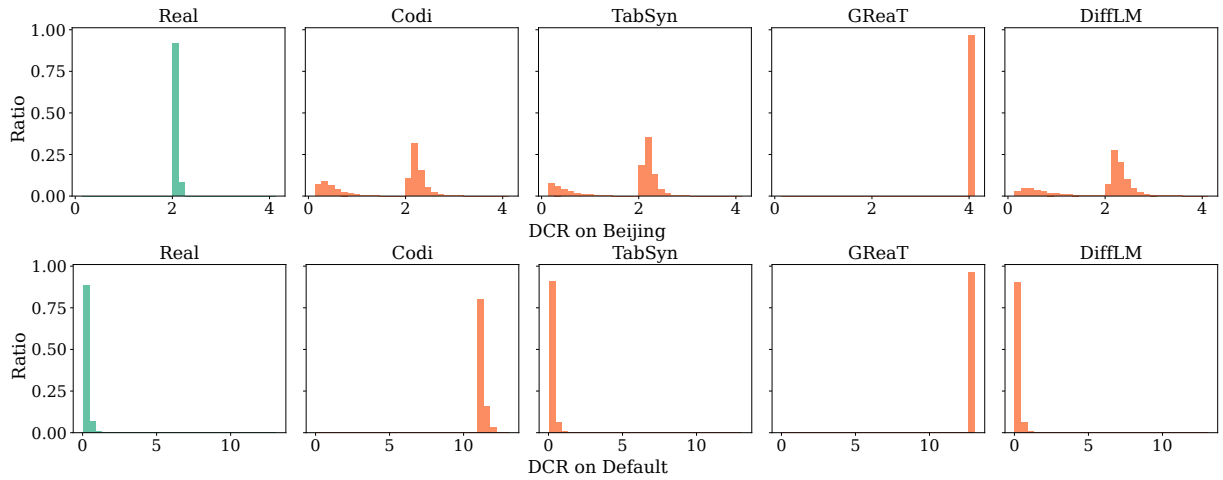


Figure 5: DCR results of the real test data, Codi, TabSyn, GReaT, and DiffLM on the *Beijing* and *Default* datasets. DiffLM exhibits a DCR distribution similar to the current SoTA method, TabSyn.

the minimum L1-distance between a synthetic data point and each training sample point:

$$\text{DCR}(x_{\text{syn}}) = \min_{x_{\text{real}} \in \mathcal{D}_{\text{train}}} L_1(x_{\text{syn}}, x_{\text{real}}). \quad (15)$$

The DCR distribution is shown in Figure 5. We observe that the LLM-based GReaT generates results that differ significantly from the training data, indicating that vanilla fine-tuning struggles to adapt LLMs to real data distributions and generate high-quality results. DiffLM demonstrates a DCR distribution similar to that of the SoTA method TabSyn on both datasets. This further indicates that our proposed general-purpose data synthesis framework can achieve performance on par with domain-specific models on specific tasks.

## C.2 Visualization

Figure 6 presents 2D t-SNE visualizations of the latent space for multiple datasets, including four

categorical tabular datasets, one numerical tabular dataset, and one tool dataset. We use DiffLM trained on the corresponding datasets to encode their validation sets, obtaining latent features. It can be observed that data of the same class encoded by DiffLM exhibit clustering characteristics in the latent space, as seen in the *Adult* and *Magic*. Notably, in the numerical dataset *Beijing*, different target values display a clear transitional distribution: the upper part of the 2D space corresponds to data with larger target values, i.e., 157 to 858, while the lower part corresponds to data with smaller target values, i.e., 1 to 23. These results demonstrate that DiffLM’s latent space learning strategy can effectively capture the real data distribution.

## C.3 DiffLM with other VAE Decoders

In Table 6, we report the tabular MLE performance of DiffLM using LLaMA3-8B as the VAE decoder.

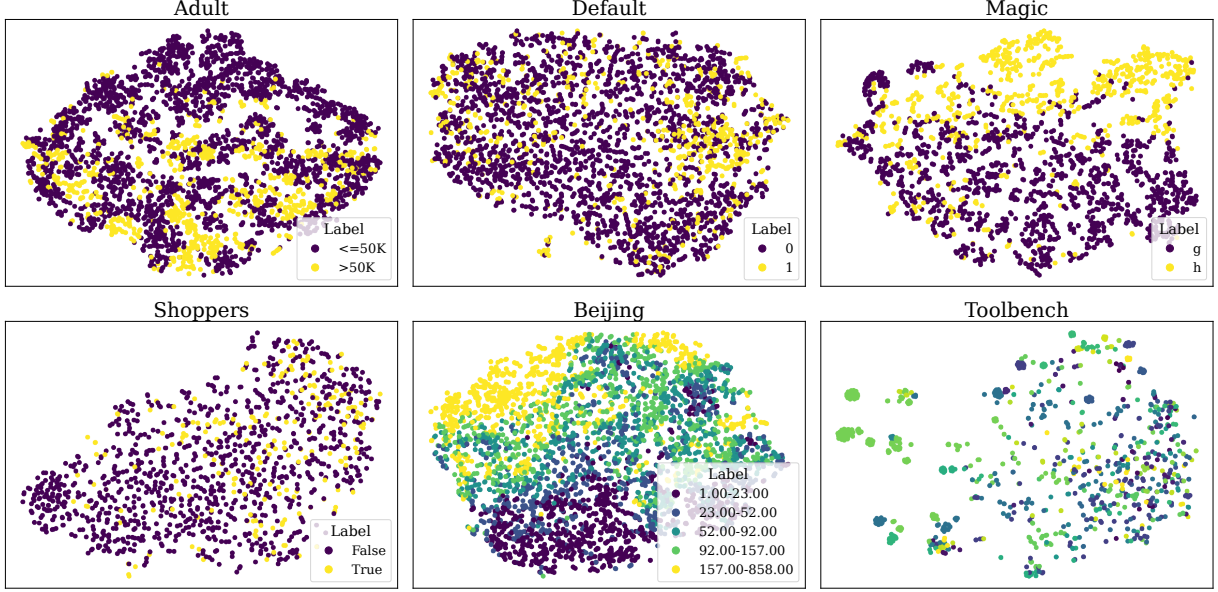


Figure 6: The t-SNE visualization of the latent space obtained by encoding evaluation data. DiffLM implicitly learns clustering relationships among different types of data.

Table 6: Tabular MLE performance with different VAE decoder models for DiffLM.

Method	Adult		Default		Magic		Shoppers		Beijing	
	MLE $\uparrow$	$\rho$ $\downarrow$	MLE $\uparrow$	$\rho$ $\downarrow$	MLE $\uparrow$	$\rho$ $\downarrow$	MLE $\uparrow$	$\rho$ $\downarrow$	MLE $\downarrow$	$\rho$ $\downarrow$
Real	0.927	-	0.770	-	0.946	-	0.926	-	0.423	-
GReaT	<b>0.913</b>	12.12	0.755	19.94	0.888	16.16	0.902	14.51	<b>0.653</b>	8.25
ICL- <i>Llama</i>	0.848	16.02	-	-	0.792	21.6	0.871	27.56	1.005	17.71
DiffLM- <i>Llama</i>	0.879	8.89	0.785	9.67	0.914	8.41	0.906	<b>6.93</b>	0.707	10.11
ICL- <i>Mistral</i>	0.803	29.22	0.732	36.00	0.881	25.64	0.882	42.00	0.865	12.45
DiffLM- <i>Mistral</i>	0.906	<b>9.74</b>	<b>0.794</b>	<b>9.06</b>	<b>0.917</b>	<b>7.53</b>	<b>0.915</b>	10.07	0.696	<b>6.35</b>

As illustrated in the table, DiffLM-LLaMA consistently outperforms the ICL-based method across all metrics and datasets. Specifically, on the *Default* dataset, while the ICL method was unable to generate valid synthetic samples, DiffLM successfully synthesized high-quality data, achieving an MLE of 0.785. This result surpasses the MLE performance of real data (0.770), clearly indicating DiffLM’s capability to produce synthetic data of superior quality compared to authentic samples. On the *Shoppers* dataset, DiffLM-LLaMA achieves an MLE of 0.906, closely approaching the 0.915 obtained by DiffLM-Mistral. Furthermore, DiffLM-LLaMA attains a rho value of 6.93, outperforming DiffLM-Mistral’s rho value of 10.07. This demonstrates that DiffLM can deliver even more favorable outcomes when integrated with more advanced language models.

#### C.4 Quantity of Synthetic Data.

We experimented with increasing the amount of data synthesized by DiffLM and combining real data with DiffLM-synthesized data. As shown in Table 7, adding more synthesized data further improves around 0.2% MLE performance in the tabular scenario. Since our method can synthesize unlimited amounts of data and we did not design any complex post-processing method, the performance improvement brought by DiffLM-synthesized data in downstream tasks still has significant room for growth. Additionally, combining real and synthetic data generated by DiffLM can improve downstream performance; all results exceed  $> 0.2\%$  of those using only DiffLM data. Notably, on the Beijing and Shoppers datasets, the combination of real data and DiffLM synthetic data surpasses 0.6%-3% of



Table 7: Tabular MLE performance with varying quantity of real and synthetic data. Performance on the Beijing dataset is evaluated using the RMSE metric, where lower values indicate better performance. 2x means we use double training synthesized data for evaluation.

	Adult	Default	Magic	Shoppers	Beijing
Real	0.927	0.770	0.946	0.926	0.423
TabSyn (SoTA)	0.915	0.764	0.938	0.920	0.582
<b>DiffLM (1x)</b>	0.894	0.793	0.910	0.9122	0.717
<b>DiffLM (2x)</b>	0.896 (+0.002)	0.795 (+0.002)	0.914 (+0.004)	0.9124 (+0.0002)	0.704 (-0.013)
<b>Real+DiffLM</b>	0.925	<b>0.802</b>	0.936	<b>0.932</b>	0.494

the performance of training on real data alone.

Table 8: The human evaluation results on 100 pairs of randomly selected DiffLM-generated tool and real tool within the same category. Averaged by 3 human experts with computer science knowledge.

	Percentage
DiffLM Win	88%
Equal	6%
Real Win	6%

### C.5 Human Evaluation.

We have used GPT-4 to rate and perform preference judgments on synthesized tools and real tools. The results in Figure 2 and Table 3 demonstrate the quality of our synthesized data. As per your suggestion, we have conducted human evaluations on the tools data. Specifically, we compared 100 pairs of randomly selected DiffLM-generated data and real data within the same category. As shown in Table 8, our synthetic data is preferred by human annotators.

### C.6 More Result of Baselines

**GReaT.** We attempted to validate the GReaT method on Mistral but found it could not directly and effectively generate data with the desired structure. GReaT organizes tabular data in a “key is value” format and uses a smaller PLM (i.e., GPT-2) for continued pretraining. However, when applied to larger models like Mistral, GReaT struggled to effectively generate the desired structured data. The sample generated by GReaT with Mistral is shown in Figure 9. We hypothesize that controlling an LM by fine-tuning it with supervised data cause catastrophic forgetting for LLMs, as sug-

gested by Luo et al. (2023b). Specifically, the “key is value” data constructed by the GReaT method, when used to continue pre-training Mistral, causes internal knowledge collapse - both undermining the model’s existing knowledge and failing to do effective data synthesis. Additionally, training the adult dataset on GReaT for 200 epochs (default settings) requires approximately 50 hours on 8 A100 80G GPUs, which is resource-intensive. In contrast, DiffLM under the same training settings requires only about 7 hours.

**TabSyn.** We want to emphasize that our goal is a unified structured data synthesis framework that supports various domains like tabular data, codes, and tools, and tabular data generation in our work is just a subdomain of synthetic data generation. As a comparison, TabSyn is not applicable to more complex data synthesis tasks, such as code generation and real-world tool generation, which involve generating longer content, more complex data types, and highly structured data, while our DiffLM can handle complicated scenarios. The results of tabular data synthesis are to demonstrate that our method possesses generality and can achieve on-par results with domain-specific models without being specifically tailored to a particular domain.

### C.7 Synthetic Data Generated by DiffLM

In Table 9, we show the samples from the *Adult* dataset with the generated tabular rows from GReaT and DiffLM method. As discussed in Section 5, DiffLM produces more diverse samples that more closely align with the real data distribution. Specifically, for columns like *workclass* and *native-country*, the outputs generated by the GReaT model are relatively homogeneous.

Table 9: Comparison of real samples and synthetic data.

Methods	age	workclass	education	occupation	race	sex	native-country	income
<b>Real</b>	40	Private	Some-college	Machine-op-inspct	Asian-Pac-Islander	Female	Japan	> 50K
	38	Private	HS-grad	Other-service	White	Female	Canada	<= 50K
	59	Private	HS-grad	Craft-repair	White	Male	England	> 50K
	29	Self-emp-not-inc	Assoc-voc	Adm-clerical	White	Male	United-States	<= 50K
	26	Private	Assoc-acdm	Prof-specialty	White	Female	Canada	<= 50K
<b>GReaT</b>	27	Private	Bachelors	Prof-specialty	White	Male	United-States	<= 50K
	22	Private	HS-grad	Craft-repair	Black	Male	United-States	<= 50K
	41	Private	HS-grad	Sales	Black	Male	United-States	<= 50K
	35	Private	HS-grad	Adm-clerical	White	Female	United-States	<= 50K
	54	Private	Doctorate	Prof-specialty	Asian-Pac-Islander	Male	India	> 50K
<b>DiffLM</b>	34	Private	Some-college	Craft-repair	White	Male	Canada	<= 50K
	53	Local-gov	Some-college	Other-service	White	Female	Canada	<= 50K
	23	Private	Bachelors	Adm-clerical	White	Male	England	<= 50K
	24	?	Some-college	?	Asian-Pacific-Islander	Male	Canada	<= 50K
	32	Local-gov	Bachelors	Adm-clerical	Asian-Pac-Islander	Male	India	> 50K

Given a API, evaluate it and assign a score from 0 to 10, with 10 being the highest quality and 0 being the lowest. Consider the aspects listed below when evaluating the API. Provide your reasoning in "reason" and include the "score" in JSON format.

Evaluation Aspects:

1. Clarity and Completeness of the Tool Description: Does the tool\_description clearly and thoroughly explain the purpose and functionalities of the tool?
2. Specificity and Accuracy of the API Name and Description: Is the api\_name descriptive and appropriate? Does the api\_description accurately and specifically describe what the API does?
3. Parameter Definition and Completeness: Are the parameters well-defined, including types, properties, and required fields? Do they cover all necessary inputs for the API to function effectively?
4. Consistency Between Tool and API Descriptions: Is there a logical connection between the tool\_description and the api\_description? Do they complement each other to provide a full understanding of the API's capabilities?
5. Ease of Integration and Use: Based on the provided information, how easy would it be for a developer to integrate and use the API? Are there any missing details that could hinder implementation?
6. Overall Usefulness and Applicability: Considering potential use cases, how valuable is the API? Does it meet the needs of its intended audience?

Instructions:

- For the API, analyze it based on the evaluation aspects.
- Summarize your findings and reasoning in a clear and concise manner in "reason".
- Assign a final score between 0 and 10, reflecting the overall quality of the API in "score" field.
- Present the output in JSON format.

API:

{api\_data}

Now, provide your answer.

Figure 7: Evaluation prompt for single-tool quality. Used by GPT-4 with temperature=1.0.

Given two sets of tools under the same category, you need to determine better\_set by following these rules:

1. Comprehensiveness of Covered Functions: Evaluate which set covers more relevant and essential functions within the category.
2. Accuracy of Tool Descriptions: Check if the tool descriptions are clear, precise, and accurately reflect each tool's functionality.
3. Difficulty of Calling the Tools: Assess the complexity involved in using the tools, considering the inputs and outputs required.
4. Overall Quality Assessment: Consider any additional factors that may impact the overall quality of the tool sets.

Set A:

{tool\_set\_a}

Set B:

{tool\_set\_b}

If one set is better based on the above criteria, indicate better\_set as "A" or "B". If both sets are of similar quality, indicate better\_set as "equal".

Now, provide your reasoning in "reason" and indicate "better\_set" ("A" or "B" or "equal") in JSON format.

Figure 8: Evaluation prompt for category-level preference. Used by GPT-4 with temperature=1.0.



